Published in final edited form as:
Cancer Res. 2009 September 15; 69(18): 7243–7251. doi:10.1158/0008-5472.CAN-09-0167.

Glioma Tumor Stem-Like Cells Promote Tumor Angiogenesis and Vasculogenesis via Vascular Endothelial Growth Factor and Stromal-Derived Factor 1

Chris Folkins[1,2], **Yuval Shaked**[3], **Shan Man**[1], **Terence Tang**[1], **Christina R. Lee**[1], **Zhenping Zhu**[4], **Robert M. Hoffman**[5], and **Robert S. Kerbel**[1,2]

[1]Department of Molecular and Cellular Biology Research, Sunnybrook Health Sciences Centre, University of Toronto, Toronto, Ontario, Canada

[2]Department of Medical Biophysics, University of Toronto, Toronto, Ontario, Canada

[3]Technion-Israel Institute of Technology, Haifa, Israel

[4]ImClone Systems, New York, New York

[5]AntiCancer, Inc., San Diego, California

Abstract

Cancer stem cells (CSC) are predicted to be critical drivers of tumor progression due to their self-renewal capacity and limitless proliferative potential. An emerging area of research suggests that CSC may also support tumor progression by promoting tumor angiogenesis. To investigate how CSC contribute to tumor vascular development, we used an approach comparing tumor xenografts of the C6 glioma cell line containing either a low or a high fraction of CSC. Compared with CSC-low tumors, CSC-high tumors exhibited increased microvessel density and blood perfusion and induced increased mobilization and tumor recruitment of bone marrow–derived endothelial progenitor cells (EPC). CSC-high C6 cell cultures also induced higher levels of endothelial cell proliferation and tubule organization *in vitro* compared with CSC-low cultures. CSC-high cultures and tumors expressed increased levels of the proangiogenic factors vascular endothelial growth factor and stromal-derived factor 1, and when signaling by either factor was blocked, all aspects of angiogenesis observed in CSC-high cultures and tumors, including microvessel density, perfusion, EPC mobilization/recruitment, and stimulation of endothelial cell activity, were reduced to levels comparable with those observed in CSC-low cultures/tumors. These results suggest that CSC contribute to tumor angiogenesis by promoting both local endothelial cell activity and systemic angiogenic processes involving bone marrow–derived EPC in a vascular endothelial growth factor–dependent and stromal-derived factor 1–dependent manner.

Introduction

Significant progress has been made in identifying stem cell-like fractions of tumor cells in a wide variety of human cancers, and characterizing their key properties, which include high

Requests for reprints: Robert S. Kerbel, Department of Molecular and Cellular Biology Research, Sunnybrook Health Sciences Centre, S-217, 2075 Bayview Avenue, Toronto, Ontario, Canada M4N 3M5. Phone: 416-480-5711; Fax: 416-480-5884; Robert.Kerbel@sri.utoronto.ca.

Note: Supplementary data for this article are available at Cancer Research Online (http://cancerres.aacrjournals.org/).

Disclosure of Potential Conflicts of Interest

R.M. Hoffman: Chief Executive Officer of AntiCancer, Inc. The other authors disclosed no potential conflicts of interest.

tumor-initiating potential, self-renewal, and multilineage differentiation capabilities, and the expression of "stemness" pathways involved in the maintenance of these properties (1). The features of the cancer stem cell (CSC) fraction suggest that they may be critical in sustaining tumor progression, and it is therefore increasingly important to further our understanding of this unique cell population and how it affects tumor biology. In this regard, an emerging area of research suggests that CSC, in addition to their proliferative capabilities, may have a role in promoting tumor angiogenesis.

A study by Bao and colleagues (2) found that the CSC-enriched $CD133^+$ fraction of human glioma cells had a significantly stronger capacity to promote angiogenesis than the CSC-depleted $CD133^-$ fraction. $CD133^+$ cells consistently yielded aggressive, highly vascularized tumors when implanted in mice, whereas $CD133^-$ cells were rarely tumorigenic and gave rise to tiny, poorly vascularized tumors. The proangiogenic capacity of the $CD133^+$ fraction was attributable to vascular endothelial growth factor (VEGF) activity. Other studies are consistent with the results of Bao and colleagues and further suggest a proangiogenic role for CSC. For example, $CD133^+$ CSC from the U87 human glioblastoma cell line expressed more VEGF and gave rise to more angiogenic xenograft tumors compared with their $CD133^-$, non-stem-like counterparts (3). CSC-enriched spheroid cultures of the MCF7 human breast cancer cell line have also been reported to express more VEGF than matched monolayer cultures with a lower CSC fraction (4). Similarly, CSC-enriched neurospheres derived from the GL261 murine glioma cell line express more VEGF and display a more proangiogenic expression signature based on microarray analysis compared with adherent, CSC-low GL261 cultures (5).

Tumor vascular development is a multifactorial process, incorporating both sprouting angiogenesis, in which tumor-derived factors promote nascent capillary formation by endothelial cells in the local tumor microenvironment, and adult vasculogenesis, in which bone marrow–derived endothelial progenitor cells (EPC) home to the tumor site, differentiate into mature endothelial cells, and incorporate into growing tumor vessels (6–13). Additionally, several other bone marrow–derived cell (BMDC) types can be recruited to sites of active angiogenesis, where they may promote angiogenesis in a paracrine manner (6, 14–19). To gain a more thorough understanding of how CSC contribute to blood vessel growth in tumors, we investigated how the stem-like cell fraction from the rat C6 glioma cell line influences tumor angiogenesis, endothelial cell organization and proliferation, and mobilization and recruitment of BMDC.

Materials and Methods

Cell culture

C6 (American Type Culture Collection) were maintained as monolayers [CSC-low, serum-containing (Ser+) condition] or nonadherent tumor spheres [CSC-high, serum-free supplemented (SFS) condition] as described (20). Human umbilical vein endothelial cells (HUVEC; Cambrex Bioscience Walkersville) were maintained as described (21). Adherent cells were harvested with 0.25% trypsin-0.03% EDTA (Invitrogen), and tumor spheres were dissociated by mechanical trituration.

Mice and tumor xenografts

For most experiments, 6- to 8-week-old female athymic nude mice (Harlan) were injected s.c. with 2×10^6 C6 cells in 200 μL serum-free DMEM.

Tumor sphere-forming assay

Tumor sphere-forming assay was done as described (21).

Limiting dilution tumor initiation assay

Nude mice were injected with 100, 1000, 5000, 10,000, or 50,000 C6 cells. Mice were monitored for 3 months and scored as positive (palpable tumor) or negative.

Immunofluorescent staining of cytospins and tumor sections

For cytospins, 100,000 cells in DMEM + 10% fetal bovine serum were loaded in Shandon cytofunnels (Fisher Scientific) and cytocentrifuged onto glass microscope slides. Tumors were frozen over dry ice in Tissue-Tek OCT (Miles) and sectioned (5–8 μm). Cells/tissues were fixed in 4% paraformal-dehyde and blocked with 10% goat serum. Antibodies were diluted in DAKO antibody diluent, and incubations were done at room temperature. Where indicated, cells/tissues were counterstained with 1 μg/mL 4′,6-diamidino-2-phenylindole (Molecular Probes). Images were acquired using a Zeiss Axioplan 2 with Zeiss Axiocam and Axio Vision 4.6.3 software and analyzed using Adobe Photoshop 6.0.

Antibodies

Antibodies used include purified mouse anti-rat nestin (1:100; BD Biosciences) with Texas red–conjugated goat anti-mouse secondary (1:200; Jackson ImmunoResearch Laboratories), rat anti-mouse CD31 (1:100; BD Biosciences) with Cy3-donkey anti-rat secondary (1:200; Jackson ImmunoResearch Laboratories), and rabbit polyclonal anti-VEGF (1:50) or anti–stromal-derived factor 1 (SDF1; 1:50; Santa Cruz Biotechnology) with Cy3-goat anti-rabbit secondary (1:100; Jackson ImmunoResearch Laboratories).

Perfusion assay

Mice were injected i.v. with 40 mg/kg Hoechst 33342 (Sigma) in PBS. After 1 min, mice were euthanized and tumors were excised, sectioned, and imaged as above.

Generation of C6 conditioned medium

C6 cells were plated in DMEM + 2% fetal bovine serum at 1.25×10^6/mL and incubated at 37°C. After 24 h, culture medium was harvested and spun down, and supernatants were stored at −80°C.

Endothelial cell proliferation assays

HUVEC were plated at 3,000 per well in 200 μL HUVEC medium in 1% gelatin-coated 96-well microplates and allowed to attach overnight. C6 conditioned medium was supplemented with 10 units/mL heparin, and aliquots were supplemented with 1,000 μmol/L AMD3100, a small-molecule antagonist of the SDF1 receptor CXCR4 (ref. 22; Sigma), or 100 μg/mL IMC1121-b, a monoclonal anti-human VEGF receptor (VEGFR) 2 antibody (ref. 23; ImClone Systems). HUVEC were incubated with 100 μL/well conditioned medium ± drug at 37°C for 18 h, after which cells were pulsed with 2 μCi [^{3}H]thymidine for 6 h.

Endothelial cell tubule formation assays

C6 conditioned medium was supplemented with 10 units/mL heparin and 10% fetal bovine serum, and aliquots were supplemented with 200 μmol/L AMD3100 or 100 μg/mL IMC1121-b. HUVEC were suspended in conditioned medium ± drug at 100,000/mL, and 300 μL/well were plated on Matrigel-coated Lab-Tek II 8-well chamber slides (Nunc) and incubated at 37°C for 20 h. Images were acquired using a Zeiss Axioplan 2 (bright-field, ×100) with attached Zeiss Axiocam and Axio Vision 4.6.3 software, and tubule length was measured using ImageJ image analysis software (NIH).

ELISA and Western blotting

Conditioned medium was analyzed undiluted using Quantikine mouse VEGF ELISA kit (R&D Systems) according to the manufacturer's instructions. For Western blotting, whole-cell lysates were prepared as described (24). Proteins from conditioned medium samples were precipitated by mixing 1 mL:5 mL with methanol and incubating for 1 h at −80°C, pelleted, and dried. Western blotting done as described (24).

Bone marrow reconstitution

Bone marrow cells harvested from femurs of athymic nude-green fluorescent protein (GFP) mice (ref. 25; Fig. 4*C* and *D*; AntiCancer) or UBI-GFP/BL6 mice (Figs. 4*B* and *C* and 6*C*; The Jackson Laboratory) were injected into the tail veins of lethally irradiated (900 rads), 6- to 8-week-old female athymic nude mice (Harlan; 10^7 cells per mouse). Mice were used in subsequent experiments after 8 weeks to allow for reconstitution.

Visualization of tumor vessel–associated BMDC

Sections of tumors grown in GFP bone marrow–reconstituted mice were stained for CD31 as above and visualized using a Zeiss Axiovert 100 with LSM510 confocal imaging system and Zeiss Advanced Imaging Microscopy software.

Flow cytometry

Circulating EPC were evaluated using flow cytometry as described (26). For analysis of tumor-recruited BMDC, single-cell suspensions were prepared as above. Cells were stained according to the antibody manufacturer's instructions. Tumor-recruited bone marrow–derived endothelial cells were defined as $GFP^+/VEGFR2^+/CD31^+/CD45^-$, recruited bone marrow–derived circulating cells (RBCC)/hemangiocytes as $CXCR4^+/CD11b^+/VEGFR1^+/CD45^+$, and Tie2-expressing monocytes (TEM) as $Tie2^+/CD11b^+/VEGFR1^+/CD45^+$. At least 50,000 events per sample were acquired, and at least 100 events were acquired in the final gate of each experiment. All antibodies were purchased from BD Biosciences.

VEGF and SDF1 blocking experiments *in vivo.*

Mice with palpable C6 tumors (7–12 days post-implantation) were treated for 2 weeks with the anti-mouse VEGFR2 blocking monoclonal antibody DC101 (ref. 27; ImClone Systems; in PBS, 800 μg/mouse/3 days i.p.) or AMD3100 (in PBS, 5 mg/kg/d s.c.). Control animals received PBS.

Statistical analysis

Histograms represent mean ± SE. Asterisks in figures denote analysis versus matched CSC-low groups (Student's *t* test): ***, $P < 0.001$; **, $P < 0.01$; *, $P < 0.05$.

Results

C6 tumor sphere cultures are enriched in CSC and give rise to CSC-enriched xenograft tumors

Previous studies on the proangiogenic nature of CSC, such as the one by Bao and colleagues (2), have compared fluorescence-activated cell sorting–sorted CSC and non-CSC populations. One difficulty with this approach is that, as Bao and colleagues reported, the non-CSC population rarely gives rise to tumors, and when it does, they are extremely growth-limited and poorly vascularized. Although in this situation it is tempting to conclude that the non-CSC-derived tumors are poorly vascularized due to lack of angiogenic capacity in the non-CSC fraction, it is also possible that, due to its inherent lack of proliferative

potential, the non-CSC fraction failed to drive tumor growth to a point where the angiogenic switch was initiated. To avoid such difficulties in the interpretation of our results, we used an approach comparing the angiogenic properties of size-matched, progressively growing tumors with either low or high CSC content to study how the CSC fraction influences tumor vascular development.

The C6 rat glioma cell line contains a CSC fraction that can be expanded by prolonged culture in serum-free medium (20). We took advantage of this property and generated long-term C6 cultures grown either as monolayers in serum-containing media (Ser+ condition) or as nonadherent tumor spheres in serum-free medium (SFS condition) supplemented as described (20). Consistent with the results of Kondo and colleagues (20), our C6 SFS cultures were significantly enriched in CSC compared with the C6 Ser+ cultures as evidenced by increased formation of tumor spheres at clonal density in serum-free conditions (Fig. 1*A*), increased expression of the neural precursor marker nestin (Fig. 1*B*), and increased tumor-initiating capacity when implanted s.c. in nude mice at limiting dilution (Table 1). The difference in tumor-initiating capacity was only noticeable when 5,000 cells were injected. A possible explanation for this is that, at the next highest dilution (10,000 cells), there is a sufficient number of tumorigenic cells in both groups to initiate a tumor and, at the next lowest dilution (1,000 cells), there is an insufficient number of tumorigenic cells in either group. Another possible contributing factor is that, at the lowest dilutions in our assay, the likelihood that sufficient numbers of tumorigenic cells remain healthy throughout the xenotransplant process and retain their ability for tumor “take” is reduced. Ser+- and SFS-derived tumors grew at similar rates when 5,000 or 10,000 cells were injected, although, when 50,000 cells were injected, the growth rate of Ser+-derived tumors was somewhat faster, and this difference was statistically significant (Supplementary Fig. S1). This difference in growth rate may be reflective of the slower cycling time associated with stem-like cells.

After 4 weeks of tumor growth, cells from dissociated SFS-derived tumors still formed significantly more tumor spheres at clonal density than cells from Ser+-derived tumors (Fig. 1*C*), indicating that CSC-low (Ser+) and CSC-high (SFS) cultures give rise, respectively, to tumors that maintain a sustained low or high fraction of self-renewing CSC.

Tumor volume matching

To account for the noted difference in growth rate, in each subsequent *in vivo* experiment where CSC-low and CSC-high tumors are compared, tumors were selected such that the average tumor volume between groups was not significantly different.

Increased vessel density and blood perfusion in CSC-high tumors

To determine the effect of the CSC fraction on tumor angiogenesis, Ser+ or SFS cells were implanted s.c. in nude mice. After 3 weeks, tumor microvessel density and blood perfusion were assessed. Both microvessel density (Fig. 2*A, top, b*) and perfusion (Fig. 2*A, bottom, c*) were significantly higher in CSC-high tumors, suggesting that the CSC fraction has a role in promoting tumor vascular development.

Increased promotion of endothelial cell proliferation and tubule formation by CSC-high cultures

To gain insight into the mechanisms underlying the increased angiogenesis observed in CSC-high tumors, we investigated the effects of secreted factors from CSC-low and CSC-high C6 cultures on vascular endothelial cells *in vitro*. HUVEC were plated with either CSC-low or CSC-high conditioned medium, and proliferation was measured by radio-labeled thymidine incorporation assay. Similarly, HUVEC were plated on Matrigel with C6

conditioned medium to assess formation of capillary-like tubule networks. Higher degrees of both endothelial cell proliferation (Fig. 3*A* and *B*) and tubule formation (Fig. 3*C*) were promoted by CSC-high conditioned medium, suggesting that CSC may promote angiogenesis in part by stimulation of endothelial cell activity.

Increased endothelial progenitor mobilization and BMDC recruitment in mice with CSC-high xenograft tumors

Another contributing factor to tumor vascular development is the recruitment of various proangiogenic BMDC populations. These include EPC, which enter the circulation in response to tumor-derived proangiogenic factors and home to the tumor where they can incorporate into nascent capillaries (6–13). Other BMDC, including RBCC/hemangiocytes (14, 15), TEM (16, 17), tumor-associated dendritic cells (18), and tumor-associated stroma cells (19), have been found to home to perivascular sites, where they may contribute to vascular development in a paracrine manner. To investigate whether CSC also have a role in BMDC-driven proangiogenic processes, we evaluated EPC mobilization and tumor recruitment of various BMDC populations in mice bearing CSC-low or CSC-high tumors.

Mice with CSC-high tumors had significantly higher levels of circulating EPC than mice with CSC-low tumors (Fig. 4*A*; Supplementary Fig. S2), suggesting a role for CSC in mobilizing EPC. To evaluate and visualize BMDC recruitment, lethally irradiated nude mice were reconstituted with bone marrow from GFP^+ donors and implanted with CSC-low or CSC-high tumors. Tumor sections were stained with a fluorescent-tagged antibody to the vascular marker CD31, and vessel-associated BMDC (GFP^+ cells within $CD31^+$ microvessels) were visualized by confocal microscopy. The fraction of microvessels with associated BMDC was not significantly different between CSC-low and CSC-high tumors (Fig. 4*B*). With this methodology, we are potentially visualizing several different BMDC populations simultaneously, which may mask significant differences in recruitment of specific BMDC subpopulations between CSC-low and CSC-high tumors. Therefore, we employed a second approach to evaluate recruitment of specific BMDC subpopulations.

To evaluate recruitment of EPC, RBCC/hemangiocytes, and TEM, flow cytometry was used on dissociated tumors from GFP-bone marrow–reconstituted mice to identify BMDC (GFP^+) in the tumor expressing endothelial cell markers ($VEGFR2^+/CD31^+/CD45^-$ to identify recruited, matured EPC) or markers for RBCC/ hemangiocytes ($CXCR4^+/CD11b^+/VEGFR1^+/CD45^+$) or TEM ($Tie2^+/CD11b^+/VEGFR1^+/CD45^+$). There was no significant difference in recruitment of RBCC/hemangiocytes or TEM between CSC-low and CSC-high tumors (Fig. 4*C*), whereas significantly higher numbers of GFP^+ endothelial cells were recruited to CSC-high tumors (Fig. 4*D*). This suggests that CSC promote homing and recruitment of EPC to the tumor. The possibility remains that CSC contribute to recruitment of other BMDC as well, although our results suggest that in our model CSC do not significantly affect recruitment of RBCC/hemangiocytes or TEM.

Increased expression of proangiogenic factors in CSC-high cultures and tumors

To further our understanding of CSC-driven angiogenic processes, we evaluated expression of two important proangiogenic factors, VEGF and SDF1, in CSC-low and CSC-high cultures and tumors. VEGF is a potent stimulator of local angiogenesis and EPC mobilization (28), and SDF1 promotes EPC recruitment and endothelial cell activity (29–31). Furthermore, we recently found that chemotherapy induces EPC mobilization mediated by systemic SDF1 induction (32). ELISA using conditioned medium showed that more VEGF was secreted by CSC-high cultures (Fig. 5*A*). SDF1 secretion was measured by Western blot of precipitated proteins from conditioned medium. Although whole-cell lysate of CSC-high cultures contained less SDF1 than CSC-low culture lysate, conditioned

medium precipitate from CSC-high culture was greatly enriched for SDF1 (Fig. 5*B*). This suggests that, in CSC-low tumors, SDF1 is not as highly secreted, so intracellular levels are higher, whereas, in CSC-high tumors, SDF1 secretion is increased, so intracellular levels are low but extracellular levels are high. Immunofluorescent staining of established CSC-low and CSC-high tumor sections showed that CSC-high tumors express significantly more VEGF (Fig. 5*C, top*) and SDF1 (Fig. 5*C, bottom*). In immunostained tumor sections, we are likely seeing an overlap of intracellular and extracellular SDF1, which may explain why the difference in magnitude of expression is less apparent than what was observed by Western blot.

CSC-derived VEGF and SDF1 are important mediators of CSC-driven angiogenesis

To evaluate the importance of VEGF and SDF1 in CSC-driven angiogenic processes, we performed blocking experiments using CSC-low and CSC-high cultures and tumors. When tumor-bearing mice were treated with the anti-mouse VEGFR2-blocking monoclonal antibody DC101 (Fig. 6*A*), or AMD3100, a small-molecule antagonist of the SDF1 receptor CXCR4 (Fig. 6*B*), CSC-high tumors no longer exhibited increased microvessel density compared with CSC-low tumors, suggesting that VEGF and SDF1 are important in establishing the “angiogenic advantage” observed in CSC-high tumors.

Because we found that CSC promote local endothelial cell activity and EPC recruitment, we investigated the importance of VEGF and SDF1 in each of these mechanisms of CSC-driven angiogenesis. When HUVEC were incubated with C6 conditioned medium and AMD3100 (Fig. 3*B*) or an anti-human VEGFR2-blocking antibody (Fig. 3*A*), CSC-high conditioned medium no longer stimulated higher levels of HUVEC proliferation than CSC-low conditioned medium. Similarly, HUVEC tubule formation in response to CSC-high conditioned medium was greatly reduced, whereas tubule formation in response to CSC-low conditioned medium was reduced to a much lesser degree by anti-VEGR2 and nearly unaffected by AMD3100 (Fig. 3*C*). These results suggest that stimulation of endothelial cell proliferation and tubule formation by CSC depends in part on VEGF and SDF1. Interestingly, VEGFR2 blockade caused a decrease in tubule formation, but not proliferation, in the CSC-low group despite that both of these processes are influenced by VEGF. Although the reason for this discrepancy is unclear, a likely explanation is that, within the conditions of our assay, tubule formation in the CSC-low group was sensitive to the amount of VEGFR2 inhibition used, whereas the baseline level of proliferation in the CSC low group was not.

DC101 dramatically reduced the increased mobilization of EPC previously observed in mice with CSC-high tumors (Fig. 4*A*). Similarly, AMD3100 reduced EPC recruitment in CSC-high tumors to levels similar to those in CSC-low tumors (Fig. 6*C*). AMD3100 had no significant effect on recruitment of RBCC/hemangiocytes or TEM (data not shown). These results suggest that VEGF and SDF1 promote CSC-driven EPC mobilization and homing/recruitment, respectively.

Discussion

The recent surge in interest in the CSC model has led to an enormous amount of research seeking to identify and characterize CSC in nearly every major disease site. This interest is largely driven by the prediction that CSC represent a critical (and previously unrecognized) therapeutic target. Specifically, the proliferative and self-renewal capabilities of CSC imply that they have important roles in initiating and sustaining tumor growth, and evidence also suggests a role in metastasis (1). Our work suggests that CSC may have a role in yet another critical element of tumor progression, that is, tumor angiogenesis. We show that tumors with a high CSC content are more strongly angiogenic and that this results from increased local

endothelial cell activity as well as mobilization and homing/recruitment of bone marrow–derived EPC, both of which are dependent on increased expression of VEGF and SDF1. Our findings are consistent with previous studies showing increased expression of proangiogenic factors and increased stimulation of angiogenesis by the CSC fraction compared with non-CSC tumor cells (2–5). These findings highlight the need for continued investigation into CSC as a potentially important target for therapy.

It may seem counterintuitive to expect that CSC, which by definition represent a very small minority of cells in a tumor, could make a significant contribution to tumor angiogenesis. It is important to note, however, that, early during tumor initiation or the seeding of a metastatic lesion, CSC would in theory represent a much higher fraction of the overall tumor cell mass. It is in these scenarios that the effect of CSC on angiogenesis may be significant. Indeed, transient bursts of angiogenic activity can be sufficient to initiate sustained tumor angiogenesis (33). Therefore, it is possible that CSC provide the signals necessary to trip the “angiogenic switch” early during the growth of primary and/or metastatic tumors. This is an interesting possibility to consider in light of recent evidence suggesting that glioma CSC are maintained by a vascular niche (34). It is logical that, as part of its ability to initiate a primary tumor or seed a metastatic lesion at distant sites with potentially suboptimal microenvironments, a CSC has the built-in capacity to promote the development of a niche to support its survival. If further research uncovers a role for CSC in the angiogenic switch, this may inform the development of new antiangiogenic therapeutic approaches aimed at, for example, disrupting CSC-derived angiogenic “bursts” during the growth of metastatic lesions.

Another circumstance in which proangiogenic capabilities of CSC may be important is during tumor regrowth following therapy. Due to properties they share with normal tissue stem cells, CSC are predicted to be resistant to many conventional cytotoxic anticancer therapies and consequently are expected to survive following therapy and drive tumor regrowth (35). Indeed, the CSC fraction is enriched following radiotherapy (36) and chemotherapy (37). The core of resistant CSC remaining after treatment represents another scenario in which CSC would make up a significant fraction of the overall tumor mass and consequently may have a significant role in supporting tumor regrowth by reinitiating angiogenesis. This concept is particularly interesting when considered in the context of recent studies from our group. We have found that, following treatment with cytotoxic agents including standard chemotherapy drugs (32) and vascular-disrupting agents (38), host-mediated systemic mobilization of EPC from the bone marrow occurs, resulting in angiogenic rebound and tumor cell repopulation. Considering the drug resistance and proangiogenic properties of CSC, it is reasonable to predict that they contribute to this observed rebound following cytotoxic therapy. Furthermore, this angiogenic rebound and associated tumor regrowth was blunted by combining antiangiogenic agents with the cytotoxic treatments (32, 38). The possibility that drug-resistant CSC contribute to the rebound process underscores the importance of using this type of combination treatment approach because multiple cycles of cytotoxic therapy would be predicted to gradually enrich the proangiogenic CSC fraction in the tumor, thereby enhancing blood vessel regrowth and tumor repopulation in the absence of a coadministered antiangiogenic agent. Following similar reasoning, one could predict that tumors with an inherently larger CSC fraction would promote a more robust vascular rebound/repopulation, making the use of antiangiogenic/cytotoxic combination therapies particularly important with such tumors. If these concepts are valid, they could inform treatment decisions in the future if it becomes possible to assess the CSC fraction a priori and possibly the development of new therapeutic strategies, such as the addition of CSC-targeted therapies to cytotoxic/ antiangiogenic combination regimens to further blunt CSC-derived proangiogenic signaling.

Our work may have additional implications for our understanding of the contribution of bone marrow–derived EPC to tumor vascular development. Many studies have suggested that EPC residing in the bone marrow can be recruited to the tumor in response to tumor-derived cytokines, where they contribute to vascular development by incorporating into the walls of nascent capillaries (6). The significance of this contribution is still a matter of considerable debate, however. Although some studies have shown a significant role for EPC in tumor angiogenesis in certain models (7–13), and previous work from our group has shown that a robust recruitment of these cells occurs following cytotoxic therapy (32, 38), in many cases, the level of EPC incorporation into tumor vessels is reported to be very low or even nonexistent (39–45), calling into question the general relevance of these cells to tumor blood vessel growth. Our work suggests that tumors with a larger CSC fraction recruit greater numbers of EPC, which raises the possibility that EPC recruitment may play a more significant role in tumor vascular development in tumors with a large CSC fraction. The correlation between CSC fraction and EPC recruitment could possibly explain some of the discrepancies in the observed levels of EPC recruitment between various studies, because the size of the CSC fraction is also reported to vary significantly between different tumor types as well as between individuals with the same tumor type (1). Further study of the relationship between CSC and EPC is warranted, as both of these cell types, although currently incompletely understood, have potentially major implications for tumor biology and therapy.

Significant work is required before we can fully understand the role of the CSC fraction in tumor angiogenesis. It will be important to study the mechanisms, timing, and extent of involvement of CSC in the various angiogenic processes, as these will all have implications for our understanding of tumor vascular development and CSC biology as well as our approach to various anticancer therapies including antiangiogenic and CSC-targeted therapies. As with many aspects of CSC biology, however, advancement in this area will depend primarily on the continued development of better models and improved techniques to better identify, isolate, and track CSC throughout tumor development.

Supplementary Material

Refer to Web version on PubMed Central for supplementary material.

Acknowledgments

Grant support: Canadian Institutes for Health Research, Canadian Cancer Society Research Institute, Ontario Institute for Cancer Research, and a sponsored research agreement with ImClone Systems (R.S. Kerbel); Canadian Institutes for Health Research doctoral research award and Ontario Graduate Scholarship (C. Folkins).

We thank Cassandra Cheng for excellent secretarial assistance.

References

1. Visvader JE, Lindeman GJ. Cancer stem cells in solid tumours: accumulating evidence and unresolved questions. Nat Rev Cancer. 2008; 8:755–68. [PubMed: 18784658]
2. Bao S, Wu Q, Sathornsumetee S, et al. Stem cell-like glioma cells promote tumor angiogenesis through vascular endothelial growth factor. Cancer Res. 2006; 66:7843–8. [PubMed: 16912155]
3. Yao XH, Ping YF, Chen JH, et al. Glioblastoma stem cells produce vascular endothelial growth factor by activation of a G-protein coupled formylpeptide receptor FPR. J Pathol. 2008; 215:369–76. [PubMed: 18523971]
4. Ponti D, Costa A, Zaffaroni N, et al. Isolation and *in vitro* propagation of tumorigenic breast cancer cells with stem/progenitor cell properties. Cancer Res. 2005; 65:5506–11. [PubMed: 15994920]

5. Pellegatta S, Poliani PL, Corno D, et al. Neuro-spheres enriched in cancer stem-like cells are highly effective in eliciting a dendritic cell-mediated immune response against malignant gliomas. Cancer Res. 2006; 66:10247–52. [PubMed: 17079441]
6. Hillen F, Griffioen AW. Tumour vascularization: sprouting angiogenesis and beyond. Cancer Metastasis Rev. 2007; 26:489–502. [PubMed: 17717633]
7. Duda DG, Cohen KS, Kozin SV, et al. Evidence for incorporation of bone marrow-derived endothelial cells into perfused blood vessels in tumors. Blood. 2006; 107:2774–6. [PubMed: 16339405]
8. Lyden D, Hattori K, Dias S, et al. Impaired recruitment of bone-marrow-derived endothelial and hematopoietic precursor cells blocks tumor angiogenesis and growth. Nat Med. 2001; 7:1194–201. [PubMed: 11689883]
9. Ciarrocchi A, Jankovic V, Shaked Y, et al. Id1 restrains p21 expression to control endothelial progenitor cell formation. PLoS ONE. 2007; 2:e1338. [PubMed: 18092003]
10. Nolan DJ, Ciarrocchi A, Mellick AS, et al. Bone marrow-derived endothelial progenitor cells are a major determinant of nascent tumor neovascularization. Genes Dev. 2007; 21:1546–58. [PubMed: 17575055]
11. Spring H, Schuler T, Arnold B, Hammerling GJ, Ganss R. Chemokines direct endothelial progenitors into tumor neovessels. Proc Natl Acad Sci U S A. 2005; 102:18111–6. [PubMed: 16326806]
12. Gao D, Nolan DJ, Mellick AS, Bambino K, McDonnell K, Mittal V. Endothelial progenitor cells control the angiogenic switch in mouse lung metastasis. Science. 2008; 319:195–8. [PubMed: 18187653]
13. Garcia-Barros M, Paris F, Cordon-Cardo C, et al. Tumor response to radiotherapy regulated by endothelial cell apoptosis. Science. 2003; 300:1155–9. [PubMed: 12750523]
14. Jin DK, Shido K, Kopp HG, et al. Cytokine-mediated deployment of SDF-1 induces revascularization through recruitment of $CXCR4^{+}$ hemangiocytes. Nat Med. 2006; 12:557–67. [PubMed: 16648859]
15. Grunewald M, Avraham I, Dor Y, et al. VEGF-induced adult neovascularization: recruitment, retention, and role of accessory cells. Cell. 2006; 124:175–89. [PubMed: 16413490]
16. De Palma M, Venneri MA, Galli R, et al. Tie2 identifies a hematopoietic lineage of proangiogenic monocytes required for tumor vessel formation and a mesenchymal population of pericyte progenitors. Cancer Cell. 2005; 8:211–26. [PubMed: 16169466]
17. Venneri MA, De PM, Ponzoni M, et al. Identification of proangiogenic TIE2-expressing monocytes (TEMs) in human peripheral blood and cancer. Blood. 2007; 109:5276–85. [PubMed: 17327411]
18. Conejo-Garcia JR, Benencia F, Courreges MC, et al. Tumor-infiltrating dendritic cell precursors recruited by a β-defensin contribute to vasculogenesis under the influence of Vegf-A. Nat Med. 2004; 10:950–8. [PubMed: 15334073]
19. Udagawa T, Puder M, Wood M, Schaefer BC, D'Amato RJ. Analysis of tumor-associated stromal cells using SCID GFP transgenic mice: contribution of local and bone marrow-derived host cells. FASEB J. 2006; 20:95–102. [PubMed: 16394272]
20. Kondo T, Setoguchi T, Taga T. Persistence of a small subpopulation of cancer stem-like cells in the C6 glioma cell line. Proc Natl Acad Sci U S A. 2004; 101:781–6. [PubMed: 14711994]
21. Folkins C, Man S, Xu P, Shaked Y, Hicklin DJ, Kerbel RS. Anticancer therapies combining antiangiogenic and tumor cell cytotoxic effects reduce the tumor stem-like cell fraction in glioma xenograft tumors. Cancer Res. 2007; 67:3560–4. [PubMed: 17440065]
22. Donzella GA, Schols D, Lin SW, et al. AMD3100, a small molecule inhibitor of HIV-1 entry via the CXCR4 co-receptor. Nat Med. 1998; 4:72–7. [PubMed: 9427609]
23. Lu D, Shen J, Vil MD, et al. Tailoring *in vitro* selection for a picomolar affinity human antibody directed against vascular endothelial growth factor receptor 2 for enhanced neutralizing activity. J Biol Chem. 2003; 278:43496–507. [PubMed: 12917408]
24. Ebos JM, Tran J, Master Z, et al. Imatinib mesylate (STI-571) reduces Bcr-Abl-mediated vascular endothelial growth factor secretion in chronic myelogenous leukemia. Mol Cancer Res. 2002; 1:89–95. [PubMed: 12496355]

25. Yang M, Reynoso J, Jiang P, Li L, Moossa AR, Hoffman RM. Transgenic nude mouse with ubiquitous green fluorescent protein expression as a host for human tumors. Cancer Res. 2004; 64:8651–6. [PubMed: 15574773]
26. Bertolini F, Paul S, Mancuso P, et al. Maximum tolerable dose and low-dose metronomic chemotherapy have opposite effects on the mobilization and viability of circulating endothelial progenitor cells. Cancer Res. 2003; 63:4342–6. [PubMed: 12907602]
27. Prewett M, Huber J, Li Y, et al. Antivascular endothelial growth factor receptor (fetal liver kinase 1) monoclonal antibody inhibits tumor angiogenesis and growth of several mouse and human tumors. Cancer Res. 1999; 59:5209–18. [PubMed: 10537299]
28. Hicklin DJ, Ellis LM. Role of the vascular endothelial growth factor pathway in tumor growth and angiogenesis. J Clin Oncol. 2005; 23:1011–27. [PubMed: 15585754]
29. Mirshahi F, Pourtau J, Li H, et al. SDF-1 activity on microvascular endothelial cells: consequences on angiogenesis in *in vitro* and *in vivo* models. Thromb Res. 2000; 99:587–94. [PubMed: 10974345]
30. Aghi M, Cohen KS, Klein RJ, Scadden DT, Chiocca EA. Tumor stromal-derived factor-1 recruits vascular progenitors to mitotic neovasculature, where microenvironment influences their differentiated phenotypes. Cancer Res. 2006; 66:9054–64. [PubMed: 16982747]
31. Reddy K, Zhou Z, Jia SF, et al. Stromal cell-derived factor-1 stimulates vasculogenesis and enhances Ewing's sarcoma tumor growth in the absence of vascular endothelial growth factor. Int J Cancer. 2008; 123:831–7. [PubMed: 18537159]
32. Shaked Y, Henke E, Roodhart JM, et al. Rapid chemotherapy-induced acute endothelial progenitor cell mobilization: implications for antiangiogenic drugs as chemosensitizing agents. Cancer Cell. 2008; 14:263–73. [PubMed: 18772115]
33. Indraccolo S, Stievano L, Minuzzo S, et al. Interruption of tumor dormancy by a transient angiogenic burst within the tumor microenvironment. Proc Natl Acad Sci U S A. 2006; 103:4216–21. [PubMed: 16537511]
34. Calabrese C, Poppleton H, Kocak M, et al. A perivascular niche for brain tumor stem cells. Cancer Cell. 2007; 11:69–82. [PubMed: 17222791]
35. Dean M, Fojo T, Bates S. Tumour stem cells and drug resistance. Nat Rev Cancer. 2005; 5:275–84. [PubMed: 15803154]
36. Bao S, Wu Q, McLendon RE, et al. Glioma stem cells promote radioresistance by preferential activation of the DNA damage response. Nature. 2006; 444:756–60. [PubMed: 17051156]
37. Dylla SJ, Beviglia L, Park IK, et al. Colorectal cancer stem cells are enriched in xenogeneic tumors following chemotherapy. PLoS ONE. 2008; 3:e2428. [PubMed: 18560594]
38. Shaked Y, Ciarrocchi A, Franco M, et al. Therapy-induced acute recruitment of circulating endothelial progenitor cells to tumors. Science. 2006; 313:1785–7. [PubMed: 16990548]
39. Machein MR, Renninger S, de Lima-Hahn E, Plate KH. Minor contribution of bone marrow-derived endothelial progenitors to the vascularization of murine gliomas. Brain Pathol. 2003; 13:582–97. [PubMed: 14655762]
40. Ruzinova MB, Schoer RA, Gerald W, et al. Effect of angiogenesis inhibition by Id loss and the contribution of bone-marrow-derived endothelial cells in spontaneous murine tumors. Cancer Cell. 2003; 4:277–89. [PubMed: 14585355]
41. Gothert JR, Gustin SE, van Eekelen JA, et al. Genetically tagging endothelial cells *in vivo*: bone marrow-derived cells do not contribute to tumor endothelium. Blood. 2004; 104:1769–77. [PubMed: 15187022]
42. Rajantie I, Ilmonen M, Alminaite A, Ozerdem U, Alitalo K, Salven P. Adult bone marrow-derived cells recruited during angiogenesis comprise precursors for periendothelial vascular mural cells. Blood. 2004; 104:2084–6. [PubMed: 15191949]
43. Peters BA, Diaz LA, Polyak K, et al. Contribution of bone marrow-derived endothelial cells to human tumor vasculature. Nat Med. 2005; 11:261–2. [PubMed: 15723071]
44. Larrivee B, Niessen K, Pollet I, et al. Minimal contribution of marrow-derived endothelial precursors to tumor vasculature. J Immunol. 2005; 175:2890–9. [PubMed: 16116175]

45. Purhonen S, Palm J, Rossi D, et al. Bone marrow-derived circulating endothelial precursors do not contribute to vascular endothelium and are not needed for tumor growth. Proc Natl Acad Sci U S A. 2008; 105:6620–5. [PubMed: 18443294]

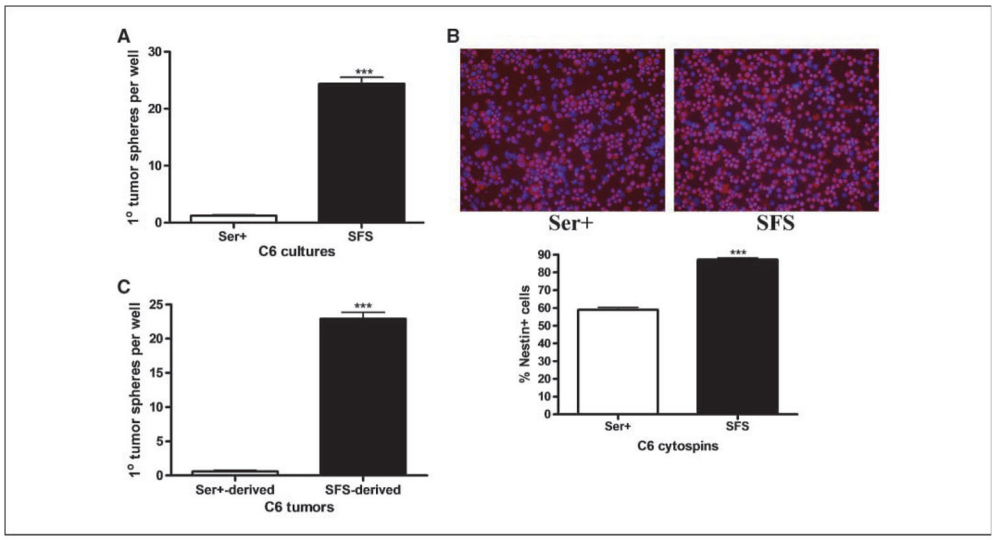

Figure 1.

Relative CSC content in C6 Ser+ and SFS cultures and tumors. *A,* tumor sphere-forming assay: 100 cells plated per well. *B,* cytospins of C6 cultures stained for nestin (Texas red; *red*). Nuclei stained with 4′,6-diamidino-2-phenylindole (*blue*), ×200. Histogram: image analysis of nestin staining. Eight fields analyzed per group. Cells displaying Texas red fluorescence above background (established using Texas red–conjugated IgG control) were counted as nestin-positive. % Nestin-positive cells per field calculated as nestin-positive cells/DAPI–stained cells (counted manually). *C, ex-vivo* tumor sphere-forming assay using established tumors (4 wk post-implantation).

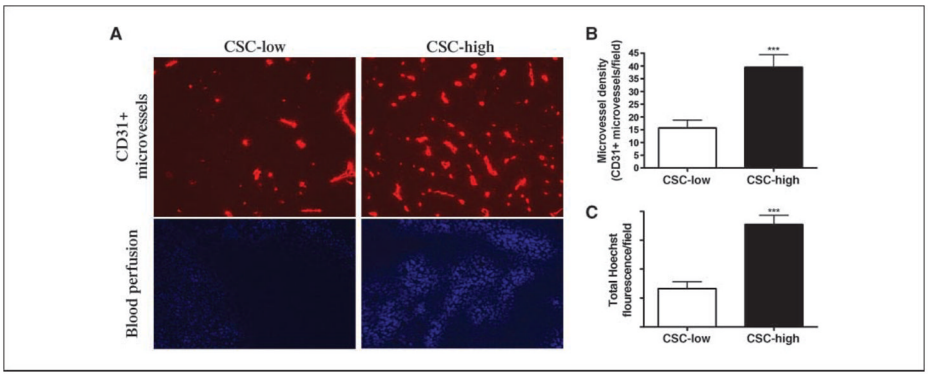

Figure 2.

Microvessel density and blood perfusion in CSC-low and CSC-high tumors. *A, top,* $CD31^+$ microvessels (Cy3; *red*), ×200; *bottom,* blood perfusion (Hoechst; *blue*), ×100. *B,* image quantification of microvessel density: number of $CD31^+$ (*red*) structures per field (counted manually). *C,* image quantification of blood perfusion: total Hoechst fluorescence intensity (total colored pixels × mean fluorescence intensity) per field. Five mice per group, five fields analyzed per tumor.

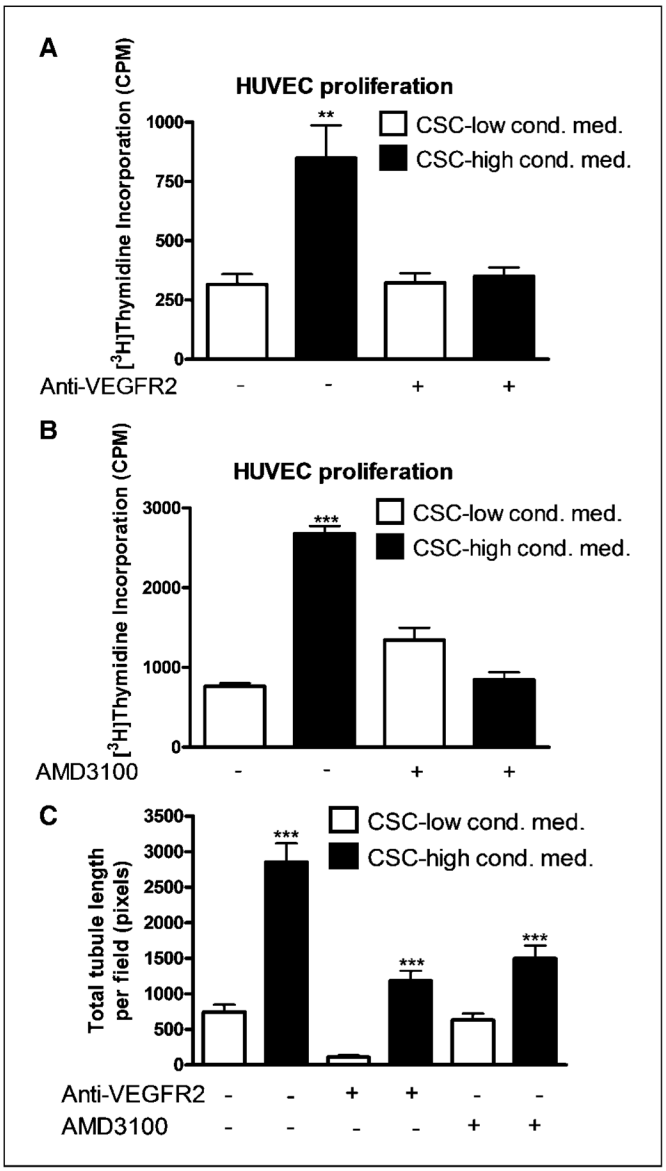

Figure 3.

Endothelial cell proliferation and tubule formation *in vitro* in response to CSC-low and CSC-high conditioned medium. *A* and *B,* HUVEC proliferation assays ± IMC1121-b (anti-VEGFR2) or AMD3100. *CPM,* counts/min, 10 wells per group. *C,* HUVEC tubule formation assays ± IMC1121-b or AMD3100. Data are the sum of lengths (in pixels) of all tubules per field at ×100. Four wells per group, 10 fields per well.

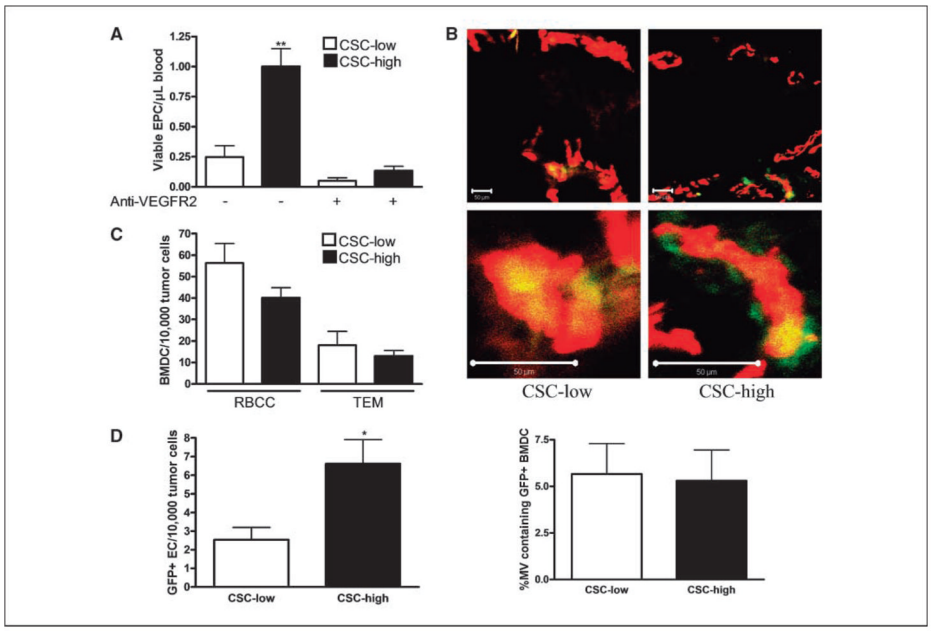

Figure 4.

EPC mobilization and vessel incorporation in mice with CSC-low and CSC-high tumors. *A,* EPC in peripheral blood ± DC101 (#/μL blood). Five mice per group. *B,* vessel-associated BMDC (GFP^+; *green*) in CD31-stained microvessels (Cy3; *red*; ×200). *Top,* full field; *bottom,* zoomed subsection. *Bar,* 50 μm. Histogram: image quantification of microvessels containing BMDC (number of GFP^+, $CD31^+$ microvessels/field divided by total number of microvessels/field; counted manually). Five mice per group, eight fields per tumor. *C* and *D,* GFP^+ RBCC/hemangiocytes, TEM (*C*), or endothelial cells (*D*), per 10,000 tumor cells, assessed by flow cytometry. Mice per group: (*C*) 8 for CSC-low and 10 for CSC-high and (*D*) 5 per group.

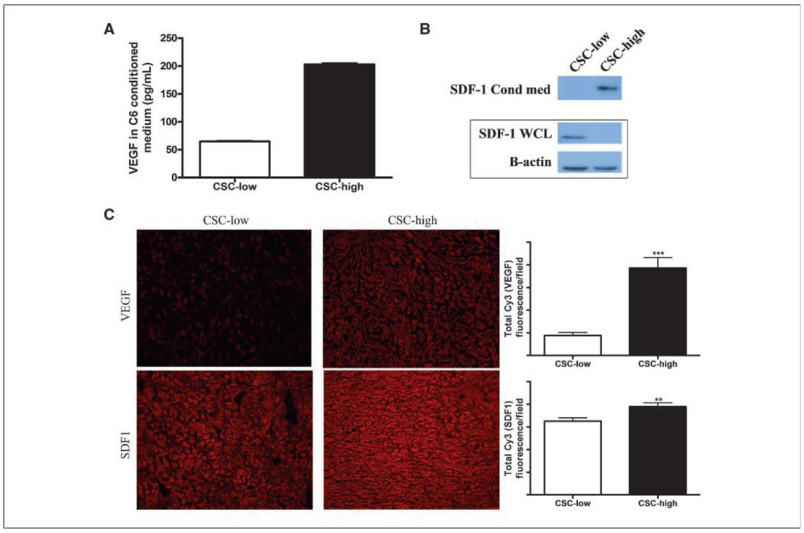

Figure 5.

VEGF and SDF1 expression in CSC-low and CSC-high cultures and tumors. *A,* ELISA for VEGF in conditioned medium. Three replicate wells per group. *B,* Western blot for SDF1 in whole-cell lysate (*WCL*; loading control: β-actin) and conditioned medium. A separate gel was used for conditioned medium. *C,* VEGF and SDF1 expression in C6 tumors. *Top,* VEGF (Cy3; *red*), ×200; *bottom,* SDF1 (Cy3; *red*), ×400. Histograms: image quantification of VEGF (*top*) and SDF1 (*bottom*). Total fluorescence = total colored pixels × mean fluorescence intensity per field. Six mice per group; VEGF: five fields per tumor and SDF1: four fields per tumor.

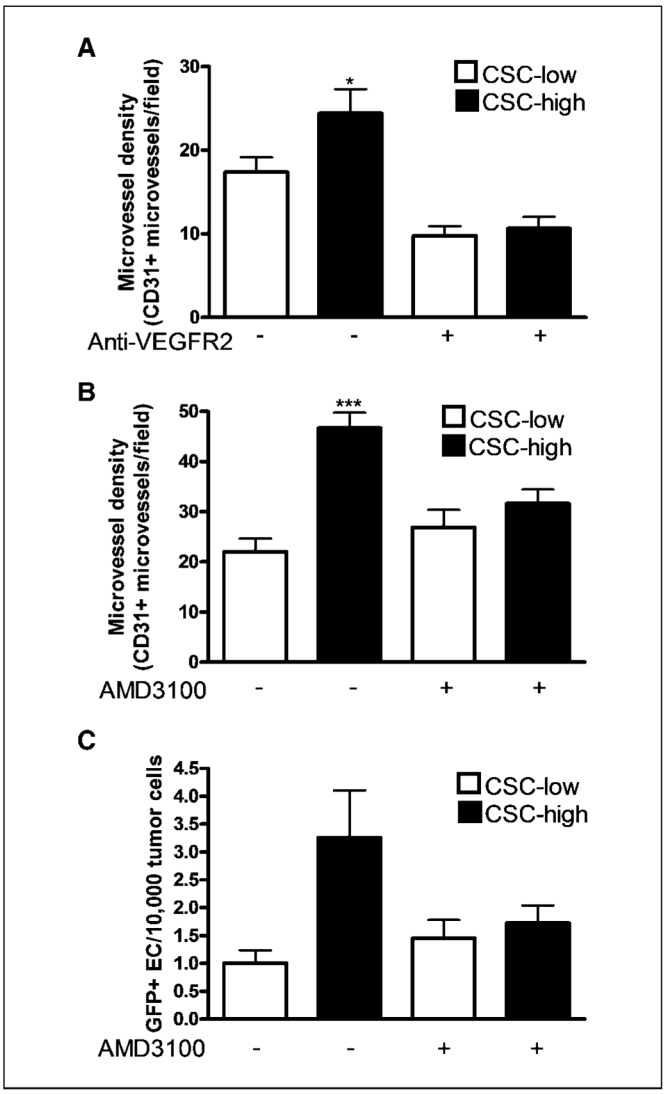

Figure 6.

VEGF- and SDF1-blocking experiments in mice with CSC-low and CSC-high tumors. *A* and *B,* image quantification of microvessel density in tumors ± DC101 (anti-VEGFR2) or AMD3100: number of $CD31^+$ structures per field (counted manually). Five mice per group, eight fields per tumor. *C,* quantification of vessel-associated, bone marrow–derived (GFP^+) endothelial cells ($CD31^+/VEGFR2^+/CD45^-$) ± AMD3100 per 10,000 tumor cells by flow cytometry. Five mice per group, except CSC-low control ($n = 3$).

Table 1

Limiting dilution tumor initiation assay

No. C6 cells injected	Tumor take (sites engrafted/injected)	
	Injecting Ser+	Injecting SFS
50,000	10/10	10/10
10,000	10/10	10/10
5,000	3/10	9/10
1,000	0/10	0/10
100	0/10	0/10

NOTE: Five mice per dilution, right and left flanks were injected, for a total of 10 injections per dilution. Results at 5,000 cell dilution are significantly different ($P = 0.0198$, Fisher's exact test).